Article ID: 1006-8775(2013) 01-0039-10

IMPACTS OF DIFFERENT KINDS OF ENSO ON LANDFALLING TROPICAL CYCLONES IN CHINA

DU Yu-gang (杜予罡), SONG Jin-jie (宋金杰), TANG Jian-ping (汤剑平)

(Key Laboratory of Mesoscale Severe Weather/Ministry of Education, and School of Atmospheric Sciences, Nanjing University, Nanjing 210093 China)

Abstract: Interannual variability of landfalling tropical cyclones (TCs) in China during 1960–2010 is investigated. By using the method of partial least squares regression (PLS-regression), canonical ENSO and ENSO Modoki are identified to be the factors that contribute to the interannual variability of landfalling TCs. El Niño Modoki years are associated with a greater-than-average frequency of landfalling TCs in China, but reversed in canonical El Niño years. Significant difference in genesis locations of landfalling TCs in China for the two kinds of El Niño phases occurs dominantly in the northern tropical western North Pacific (WNP). The patterns of low-level circulation anomalies and outgoing longwave radiation (OLR) anomalies associated with landfalling TC genesis with different types of El Niño phases are examined. During canonical El Niño years, a broad zonal band of positive OLR anomalies dominates the tropical WNP, while the circulation anomalies exhibit a meridionally symmetrical dipole pattern with an anticyclonic anomaly in the subtropics and a cyclonic anomaly near the tropics. In El Niño Modoki years, a vast region of negative OLR anomalies, roughly to the south of 25°N with a strong large-scale cyclonic anomaly over the tropical WNP, provides a more favorable condition for landfalling TC genesis compared to its counterpart during canonical El Niño years. For more landfalling TCs formed in the northern tropical WNP in El Niño Modoki years, there are more TCs making landfall on the northern coast of China in El Niño Modoki years than in canonical El Niño years. The number of landfalling TCs is slightly above normal in canonical La Niña years. Enhanced convection is found in the South China Sea (SCS) and the west of the tropical WNP, which results in landfalling TCs forming more westward in canonical La Niña years. During La Niña Modoki years, the landfalling TC frequency are below normal, owing to an unfavorable condition for TC genesis persisting in a broad zonal band from 5°N to 25°N. Since the western North Pacific subtropical high (WNPSH) in La Niña Modoki years is located in the westernmost region, TCs mainly make landfall on the south coast of China.

Key words: landfalling tropical cyclone; interannual variability; canonical ENSO; ENSO Modoki; PLS-regression

CLC number: P444 **Document code:** A

1 INTRODUCTION

China is the country most frequently affected by landfalling TCs in the world. Every year landfalling TCs cause catastrophic damage and loss of life in China. For instance, Nina, a landfalling TC in 1975, produced widespread torrential rainfall, resulting in the collapse of the Banqiao Dam and a large number of casualties that amounted to $1.2 billion in damage. In 1998, TC Herb made landfall in Taiwan and Fujian provinces, which killed about 700 people and caused $5 billion in damage.

The El Niño and Southern Oscillation (ENSO) has been proved to be responsible for the interannual variability of TC activity[1-10]. In El Niño years, more TCs generate in the southeastern WNP while less TCs formed in the northwestern WNP[1-4]. Accordingly, more intense and long-lived TCs occurred in El Niño years than in La Niña years. As for landfalling TCs in China, previous studies indicate that less TCs with stronger intensity make landfall in China in El Niño years in contrast with those in La Niña years[4-7]. The season of landfalling TCs is also shorter in El Niño years[8-10].

Recently, a new type of Pacific Ocean warming, called El Niño Modoki, has been proposed and

Received 2011-09-30; **Revised** 2012-10-19; **Accepted** 2013-01-15
Foundation item: National Natural Science Foundation of China (41105036, 41105035, 40730948, 40830958, 40921160382); National Grand Fundamental Research "973" Program of China (2009CB421502)
Biography: DU Yu-gang, Ph.D. candidate, primarily undertaking research on regional climate change, dynamics and climatology of tropical cyclones in the western North Pacific.
Corresponding author: SONG Jin-jie, e-mail: songjinjie@nju.edu.cn

investigated[11-14]. The El Niño Modoki is associated with warming in the central Pacific, while canonical El Niño is linked with warming in the eastern Pacific. These two kinds of ENSO events lead to different atmospheric circulations and result in distinctly different climate impacts[15, 16]. In recent studies, the different impacts of these two types of ENSO events on TC activities have been examined for various ocean basins. Kim et al.[17] noticed that canonical El Niño resulted in the diminishing of TCs, whereas El Niño Modoki was associated with a greater number of TCs and increasing landfall potential on North Atlantic. Chen et al.[18] found that the TC frequency was in significantly positive correlation with the ENSO Modoki index. However, the distinct effects of the two kinds of ENSO events on the TCs making landfall in China are rarely discussed.

Therefore, this study utilizes PLS-regression to identify interannual variability of landfalling TC frequency in China. Both canonical ENSO and ENSO Modoki are diagnosed to be the factors that contribute to the interannual variability of landfalling TC frequency. Furthermore, the distinct impacts of the two kinds of ENSO events on landfalling TCs are investigated and physical mechanisms possibly involved are also discussed in this study. The paper is organized as follows. Section 2 introduces the data and methods. Section 3 gives the time series of landfalling TC frequency in China, TC frequency in the WNP and the SCS, and landfalling percentage. In section 4, PLS-regression is used to diagnose the factors that contribute to the interannual variability of landfalling TC frequency in China. Effects of various ENSO phases on landfalling TC frequency and tracks are separately presented in section 5 and 6. Concluding remarks are given in section 7.

2 DATA AND METHODS

2.1 *Data*

The best-track TC data in the period 1960–2010 were obtained from the Shanghai Typhoon Institute, China Meteorological Administration (CMA). TCs that occurred in the WNP as well as the SCS with the maximum sustained wind speed greater than 17.2 m s^{-1} and ultimately made landfall in China were considered. Since about 94% of the total annual number of landfalling TCs was observed from June to October during the period 1960–2010, the present study focuses on this period [7, 18, 19].

The sea surface temperature (SST) data were from the National Oceanic and Atmospheric Administration (NOAA, USA) Extended Reconstructed SST dataset Version 3b. Its horizontal resolution is 2°×2°. The monthly wind[20] was obtained from the National Centers for Environmental Prediction/National Center for Atmospheric Research (NCEP/NCAR, USA) reanalysis datasets. The NOAA monthly OLR data[21] during the period 1974 to 2010 were also used. The horizontal resolutions of the latter two datasets are 2.5°×2.5°. The ENSO Modoki index (EMI) was delivered by Japan Agency for Marine-Earth and Technology (JAMSTEC). The NOAA Niño-3 (150–90°W, 5°S–5°N) SST index was also employed.

2.2 *Methods*

PLS-regression is a technique used to predict one or more dependent variables *Y* (predictands) with a set of independent variables *X* (predictors). It combines features from principal component analysis (PCA) and multiple linear regression. It is particularly useful when the number of predictors is larger than that of observations, and the predictors are highly correlated or even collinear. PLS-regression has been widely used in meteorology such as statistical prediction[22] and paleoclimate reconstruction[23] in recent years. Smoliak et al.[24] used this method to diagnose the factors that contribute to the interannual variability of geophysical time series, and indicated that PLS-regression may perform better than simple linear regression when the predictand time series was influenced by the predictor field through more than one pathway.

The goal of PLS-regression is to find PLS components *Z* from predictors *X* that best predict *Y*, where the PLS component is a linear combination of predictors and maximizes variance explained in predictands as well as the correlation between predictors and predictand[24]. Figure 1 shows the flow chart for PLS regression. It performs the following steps[24-26]. First, the predictors and predictands are standardized. Then the first PLS component time series z_1 is extracted from the predictors. In the next step, by using multiple linear regression, z_1 is regressed in the predictands and each of the predictors to obtain a residual predictor field and predictand time series. The procedure is repeated on the residual matrices e_x and e_y to obtain a second PLS component time series z_2, and so on. The respective PLS component time series, $z_1, z_2, \ldots z_n$, are mutually orthogonal by construction and each successive component explains a smaller amount of covariance between *X* and *Y*. The quality of the prediction obtained from PLS regression is then verified. The quality of the prediction obtained from PLS regression is evaluated with cross-validation.

In this study, the predictand y_i (i represents observations) are the frequency of TCs making landfall in China. The SST at grid points in the region (0–358°E, 40°S– 40°N) is used as the predictor x_{ij} (j is the number of grid points). In order to minimize the influence of global warming, the time series of SST at

each grid point subtracts the time series of global mean SST.

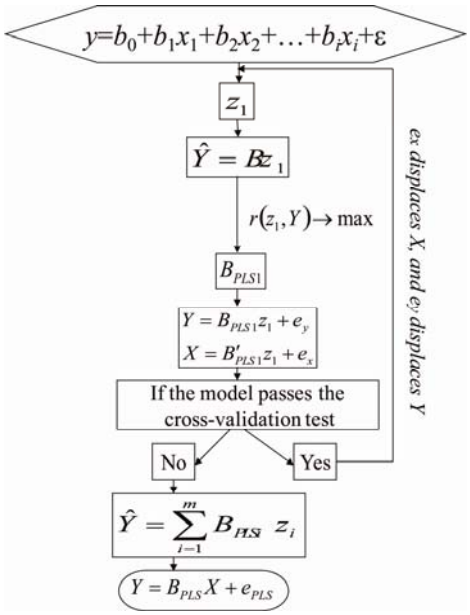

Figure 1. Flow chart for PLS regression.

3 LANDFALLING TC FREQUENCY

A total of 386 TCs made landfall in China in the typhoon season during the period 1960–2010, with an average number of 7.6 per year, while 1074 TCs formed in the WNP and the SCS with an average number of 21 per year. The mean landfalling percentage (ratio of landfalling TC number to total TC number) is 36% in China. Figure 2 shows the time series of landfalling TC frequency in China, TC frequency in the WNP and the SCS, and landfalling percentage in the typhoon season for the period 1960–2010. The maximum number of TCs making landfall in China is 12 in 1994, while 1982 and 1998 have the minimum number of 4. The time series of landfalling TC frequency exhibits large year-to-year variability. For example, in 1967 there were 11 landfalling TCs, whereas only 6 TCs made landfall in China in the next year. The long-term trend of landfalling TC frequency is indicative of a slight decrease (Figure 2a). The interannual variability is observed in both TC frequency and landfalling percentage. The frequency of TCs forming in the WNP and the SCS shows a significantly decreasing trend (Figure 2b), whereas the landfalling percentage shows an evidently upward trend (Figure 2c). The correlation coefficient between landfalling TC frequency and TC frequency is 0.57, which is statistically significant at the 95% confidence level. In other words, the number of TCs making landfall in China does not completely depend on the frequency of TCs forming in the WNP and the SCS. For instance, 20 TCs formed in the WNP and the SCS in 1981 and 1982. As for landfalling TCs, 1981 had 9 landfalling TCs, but only 4 TCs made landfall in China in 1982.

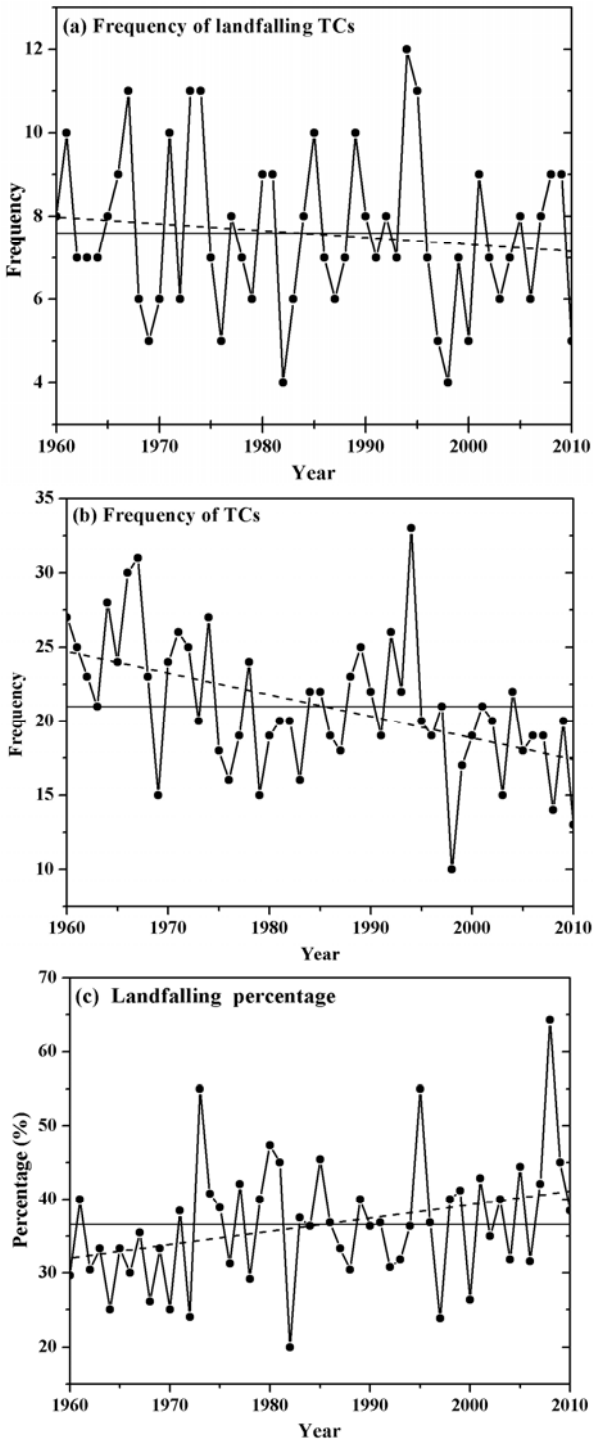

Figure 2. Time series of (a) landfalling TC frequency in China, (b) TC frequency in the WNP and the SCS, and (c) landfalling percentage in the typhoon season during the period 1960–2010. The dash lines and horizontal lines indicate the linear fit and the 1960–2010 mean, respectively.

4 DIAGNOSIS OF INTERANNUAL VARIABILITY IN LANDFALLING TC FREQUENCY

Given the large interannual variability of

landfalling TC frequency in China, PLS-regression is used to diagnose the factors that contribute to this variability. Based on the results of leave-one-out cross-validation, the leading two PLS components are statistically significant. Figure 3 shows two patterns obtained from PLS-regression, represented as a correlation coefficient between SST and the first two PLS components, respectively. The first pattern (Figure 3a), which is featured by a significantly negative center of action in eastern Pacific, primarily relates to the canonical ENSO phenomenon. It explains 25.1% of the variance of the landfalling TC frequency. The pattern associated with the second PLS component (Figure 3b) has a dominantly positive center of action in the central Pacific which closely resembles ENSO Modoki. The second PLS component explains 21.6% of the variance of the landfalling TC frequency. Since the PLS components are mutually orthogonal, the explained variances are additive. Therefore, the leading two PLS components jointly account for 46.7% of the variance of the landfalling TC frequency.

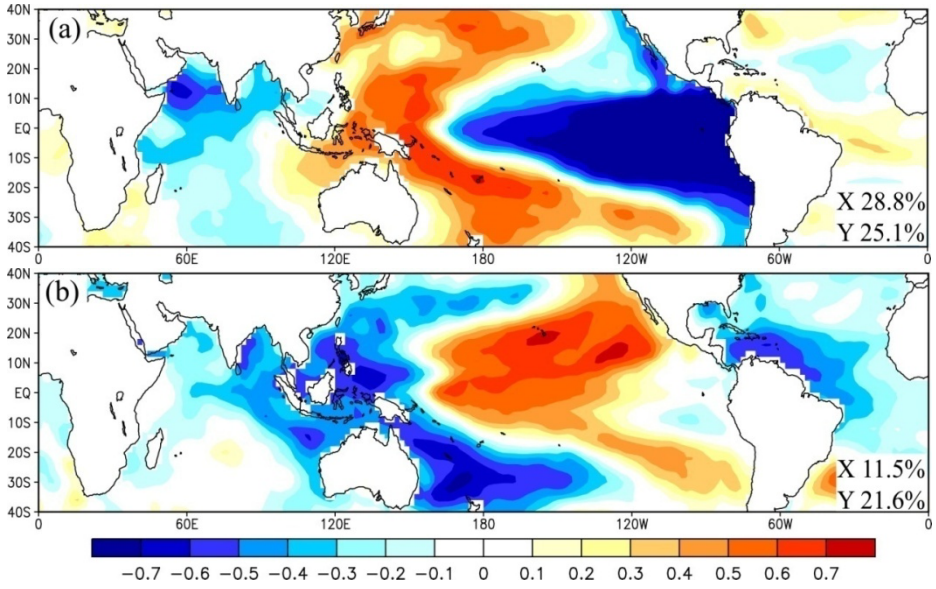

Figure 3. (a) First pattern, derived from PLS-regression analysis of June to October mean SST x_{ij} and the time series of frequency of landfalling TCs y_i, represented as the correlation coefficient between SST and the first PLS component z_1; the 95% significance level is 0.28. The fraction of variance in X and Y explained by component z_1 is shown in the lower right corner. (b) Second pattern, displayed as in Figure 3a but for the second PLS component z_2.

5 EFFECTS OF ENSO PHASES ON LANDFALLING TC FREQUENCY

Canonical ENSO and ENSO Modoki phases are defined based on the detrended SST anomaly index in the typhoon season. The Niño3 (150–90°W, 5°S–5°N) SST index, which is more (less) than one standard deviation (one negative standard deviation), is defined as the canonical El Niño (La Niña) year[17, 18]. The El Niño (La Niña) Modoki year is identified as EMI being larger (smaller) than one standard deviation (one negative standard deviation)[18]. EMI constructed by Ashok et al.[15] is defined in the following expression:

$$\mathrm{EMI} = [\mathrm{SSTA}]_{\mathrm{A}} - 0.5[\mathrm{SSTA}]_{\mathrm{B}} - 0.5[\mathrm{SSTA}]_{\mathrm{C}} \quad (1)$$

where $[\mathrm{SSTA}]_{\mathrm{A}}$, $[\mathrm{SSTA}]_{\mathrm{B}}$ and $[\mathrm{SSTA}]_{\mathrm{C}}$ represent the area-averaged SST anomalies in the regions of A (165°E–140°W, 10°S–10°N), B (110–70°W, 15°S–5°N), and C (125–145°E, 10°S–20°N), respectively. According to the above criteria, eight canonical El Niño years (1963, 1965, 1969, 1972, 1976, 1982, 1987 and 1997), eight El Niño Modoki years (1966, 1967, 1977, 1990, 1991, 1994, 2002 and 2004), ten canonical La Niña years (1964, 1970, 1971, 1973, 1975, 1985, 1988, 1999, 2007 and 2010) and two La Niña Modoki years (1983 and 1998) are chosen in this study.

5.1 *Different impacts of the two kinds of El Niño phases on landfalling TC frequency*

Table 1 lists the landfalling TC frequencies in canonical El Niño and El Niño Modoki years. Compared with the climatological mean (7.6 per year) of landfalling TC frequency during 1960–2010, seven of the eight canonical El Niño years are below normal except in 1965, whereas five-eighths of El Niño Modoki years are above normal except in 1991, 2002 and 2004. The total (average) number of landfalling TCs in canonical El Niño years is 46 (5.8) in comparison with 69 (8.6) during El Niño Modoki

years. The ratio of mean landfalling TC frequency in El Niño Modoki years to that in canonical El Niño years is 1.5:1. The difference of landfalling TC frequencies between these two kinds of El Niño phases is significant at the 99% confidence level based on the *t*-test. In general, there are more TCs making landfall in China in El Niño Modoki years than in canonical El Niño years.

Table 1. Landfalling TC frequencies during the typhoon season for canonical El Niño and El Niño Modoki years in China.

Canonical El Niño		El Niño Modoki	
Year	frequency	Year	frequency
1963	7	1966	9
1965	8	1967	11
1969	5	1977	8
1972	6	1990	8
1976	5	1991	7
1982	4	1994	12
1987	6	2002	7
1997	5	2004	7
Total/mean	46/5.8	Total/mean	69/8.6
Climatological mean	7.6	Climatological mean	7.6

Figure 4 shows the formation number and positions of TCs making landfall in China in the typhoon season during canonical El Niño and El Niño Modoki years. Table 3 presents the mean genesis positions of landfalling TCs in ENSO phases. As shown in Figure 4 and Table 3, landfalling TCs in China mainly form in the SCS (105–120°E, 5–25°N)[27] and the tropical WNP (120–180°E, 0–30°N)[18]. The mean genesis positions of landfalling TC forming in the SCS for the two kinds of El Niño phases are similar to each other. In the WNP, the mean genesis position in El Niño Modoki years is in the northwest of that in canonical El Niño years. In order to further investigate the different spatial distribution of landfalling TC genesis positions between these two types of El Niño phases, the formation area of landfalling TCs is divided into three domains: the SCS, the northern tropical WNP (N) and the southern tropical WNP (S). The latter two domains are located in the north and south of 15°N over the tropical WNP, respectively. A remarkable feature in Figure 4 is that the genesis positions of landfalling TCs in El Niño Modoki years extend more meridionally compared to its counterpart during canonical El Niño years. More accurately, there are 17 landfalling TCs forming in the SCS during El Niño Modoki years but only 11 in canonical El Niño years. In other words, the landfalling TC frequency in El Niño Modoki years is about 1.5 times that in canonical El Niño years. However, the difference in landfalling TC frequencies in the SCS between the two types of El Niño phases is not significant at the 95% confidence level based on the *t*-test. In the northern tropical WNP, the number of landfalling TCs in El Niño Modoki years is 24, which is fourfold as much as that in canonical El Niño years. The difference of landfalling TC frequencies between the two kinds of El Niño phases is significant at the 99% confidence level based on the *t*-test in this region. Furthermore, only one landfalling TC forms in the north of 20°N in canonical El Niño years, whereas the highest latitude at which the landfalling TCs generate can be 28.5°N during El Niño Modoki years. As for the southern tropical WNP, the number of landfalling TCs in canonical El Niño years (29) is almost as much as that in El Niño Modoki years (28). Therefore, the difference in landfalling TC frequencies between the two kinds of El Niño phases is a result of much more landfalling TCs forming in the northern tropical WNP during El Niño Modoki years. Moreover, a bit more TCs forming in the SCS during El Niño Modoki years also have some contributions to this difference.

In order to find out the associated physical mechanism for the impacts of different El Niño phases, the composites of OLR anomalies and 850 hPa wind anomalies in the typhoon season are examined in Figure 5 for the two El Niño phases. In El Niño Modoki years, negative OLR anomalies which enhance convection are situated in a vast region roughly extending from 120°E to the dateline and are nearly to the south of 25°N, while positive OLR anomalies that tend to suppress convection are found approximately to the north of 25°N. Meanwhile, a zonal band roughly between 0°N and 20°N is dominated by positive OLR anomalies except for the southeastern part of the tropical WNP in canonical El Niño years. Correspondingly, 850 hPa wind anomalies also show distinct patterns during different types of El Niño phases. A strong large-scale anomalous cyclone is found in El Niño Modoki years with its center near (145°E, 20°N). In contrast, the wind anomalous pattern in canonical El Niño years is characterized by a meridionally symmetric dipole. The anomalous cyclone and anomalous anticyclone prevails to the south of 25°N and the north of 25°N, respectively. More accurately, the positive OLR anomalies in the SCS are more intense in canonical El Niño years than that in El Niño Modoki years, hence

inducing a bit more landfalling TC genesis in El Niño Modoki years. In the northern tropical WNP, strongly suppressed convection with the center near (150°E, 20°N) cancels the impact of the anomalous cyclone in canonical El Niño years. Meanwhile, the anomalous anticyclone dominating north of 20°N also suppresses the formation of landfalling TCs in canonical El Niño years. Comparably, the enhanced convection accompanied by anomalous cyclones to the south of 30°N in the domain provides a favorable condition for landfalling TC genesis in El Niño Modoki years. In the southern tropical WNP, the two El Niño phases have similar patterns, which exhibit positive OLR anomalies in the west and negative OLR anomalies in the east, accompanied with prevailing low-level westerly anomalies. These patterns explain plenty of landfalling TC genesis in both of the two kinds of El Niño phases.

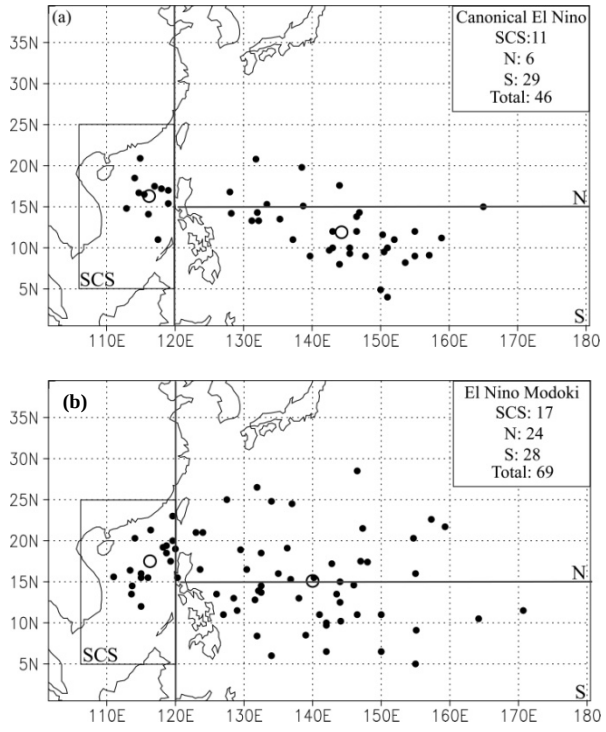

Figure 4. Formation number and positions of TCs making landfall in China during the typhoon season for (a) canonical El Niño and (b) El Niño Modoki years. The two hollow circles represent mean genesis positions in the SCS and the WNP, respectively.

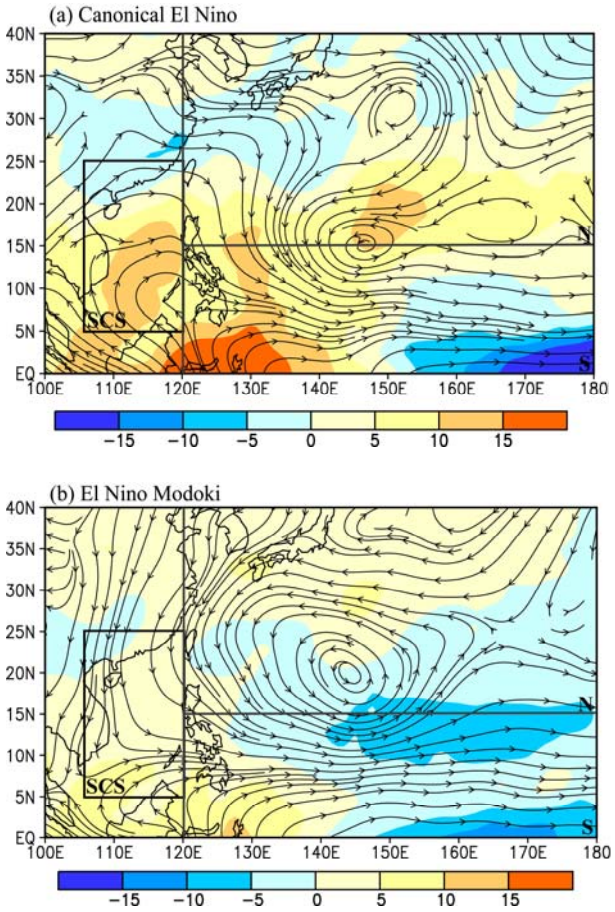

Figure 5. Composites OLR anomalies (shade: W m^{-2}) and 850 hPa wind anomalies (streamline) during the typhoon season for (a) canonical El Niño and (b) El Niño Modoki years. OLR anomalies are calculated from 1975 onwards because of the OLR data length.

5.2 *Different impacts of the two kinds of La Niña phases on landfalling TC frequency*

Table 2 gives details of the landfalling TC frequencies during canonical La Niña and La Niña Modoki years in China. The mean frequency of landfalling TCs in canonical La Niña years is 7.8 per year, which is slightly above normal. The landfalling TC frequencies of La Niña Modoki years are below normal with an average frequency of 5 per year. The ratio of mean frequency of landfalling TC in La Niña Modoki years to that in canonical La Niña years is 1:1.6. However, the difference of frequencies of landfalling TCs between these two kinds of La Niña phases is not significant at the 95% confidence level based on the *t*-test. As shown in Table 3 and Figure 6, the mean genesis position of landfalling TCs in the SCS during La Niña Modoki years is in the northeast of that in canonical La Niña years. In the tropical WNP, the mean genesis positions of the two types of La Niña phases are almost identical to each other. Moreover, landfalling TCs mainly form in the west of tropical WNP during the two kinds of La Niña phases.

Table 2. Landfalling TC frequencies during the typhoon season for canonical La Niña and La Niña Modoki years in China.

Canonical La Niña		La Niña Modoki	
Year	frequency	Year	frequency
1964	7	1983	6
1970	6	1998	4
1971	10		
1973	11		
1975	7		
1985	10		
1988	7		
1999	7		
2007	8		
2010	5		
Total/mean	78/7.8	Total/mean	10/5
Climatological mean	7.6	Climatological mean	7.6

Table 3. Mean genesis positions of landfalling TCs in canonical El Niño, El Niño Modoki, canonical La Niña and La Niña Modoki years.

	SCS		WNP	
	Latitude(°N)	Longitude(°E)	Latitude(°N)	Longitude(°E)
Canonical El Niño years	16.3	116.2	11.9	144.3
El Niño Modoki years	17.5	116.3	15.1	140.0
Canonical La Niña years	15.7	114.2	14.1	135.4
La Niña Modoki years	18.6	117.9	12.8	136.5

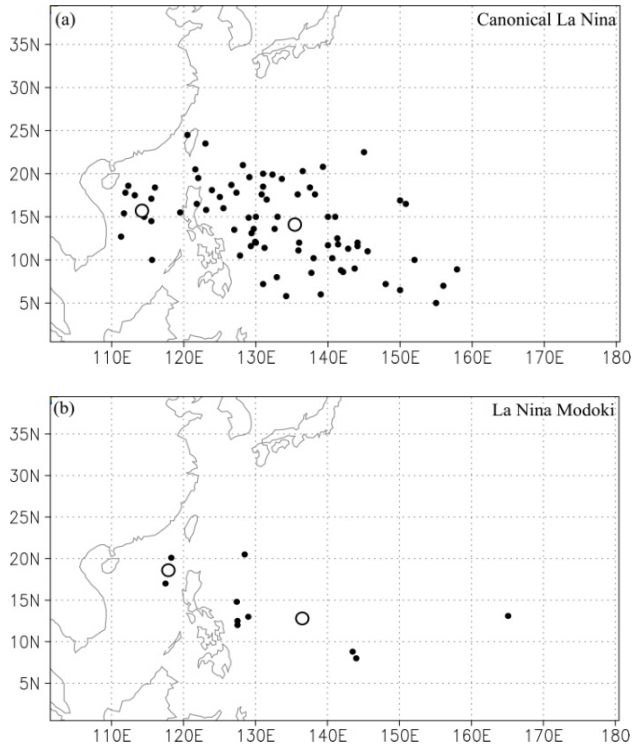

Figure 6. Formation positions of TCs making landfall in China during the typhoon season for (a) canonical La Niña, (b) La Niña Modoki years. The two hollow circles represent mean genesis positions in the SCS and the WNP, respectively.

The composites of OLR anomalies and 850 hPa wind anomalies for the two kinds of La Niña phases in the typhoon season are shown in Figure 7. In canonical La Niña years, enhanced convection prevails in the SCS and the west of tropical WNP, while suppressed convection accompanied with an anomalous anticyclone is found in the east of WNP. This pattern results in the genesis locations of landfalling TCs in China being generally more to the west than to the east in tropical WNP (Figure 6a). As for La Niña Modoki years, suppressed convection and two anomalous anticyclones almost dominate the entire landfalling TC genesis region (105–180°E, 5–25°N). This pattern provides an unfavorable condition for TC genesis.

Compared with the four ENSO phases, El Niño Modoki years have the largest number of TCs making landfall in China, while La Niña Modoki years have the smallest number of landfalling TCs in China (Tables 1 and 2). As for the genesis positions, landfalling TCs in canonical El Niño years mainly form in the SCS and the southern tropical WNP. The genesis positions of El Niño Modoki years spread in the SCS and the entire tropical WNP. In canonical La Niña years, landfalling TCs mainly form in the west of the tropical WNP. The genesis positions of landfalling TCs in La Niña Modoki years are mainly located in the southwest of the tropical WNP. Table 4 lists the mean landfalling percentages in ENSO phases. The canonical El Niño years have the minimum mean

landfalling percentage, while the La Niña Modoki years have the maximum mean landfalling percentage. In general, the mean landfalling percentages in La Niña phases are larger than in El Niño phases. A possible reason is that the genesis positions in La Niña phases are more to the west than in El Niño phases, which makes TCs easier to make landfall in China.

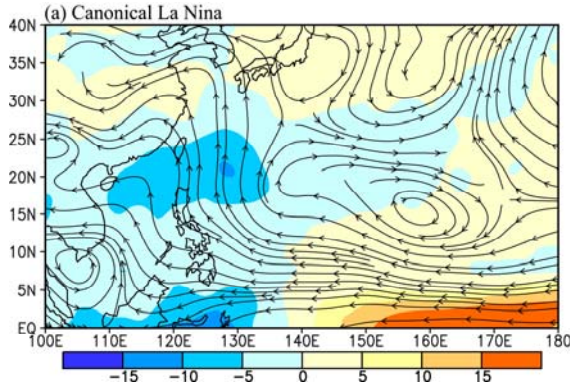

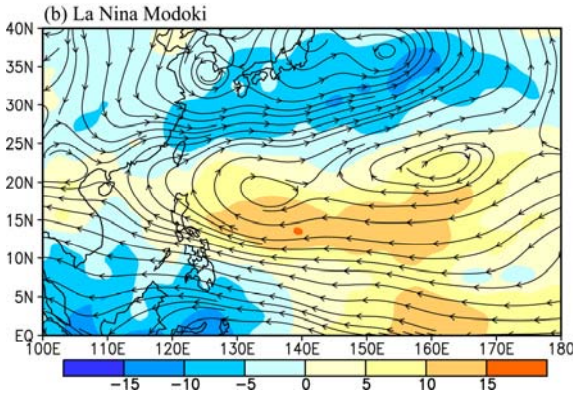

Figure 7. Composites OLR anomalies (shade: W m^{-2}) and 850 hPa wind anomalies (streamline) during the typhoon season for (a) canonical La Niña and (b) La Niña Modoki years. OLR anomalies are calculated from 1975 onwards because of the OLR data length.

Table 4. Mean landfalling percentages in ENSO phases.

	Canonical El Niño	EL Niño Modoki	Canonical La Niña	La Niña Modoki	Climatol. mean
Percentage (%)	29	35.5	38	38.8	36.6

6 IMPACTS OF ENSO PHASES ON LANDFALLING TC TRACKS

The tracks of landfalling TCs in different kinds of El Niño phases are shown in Figure 8. There are more TCs making landfall in the northern coast of China in El Niño Modoki years than in canonical El Niño years. The location and strength of the WNPSH (5870 gpm contour at 500 hPa)[29, 30] have great impacts on the tracks of TCs[1, 28, 29]. The WNPSH in the typhoon season for various ENSO phases is examined in Figure 10. The locations of WNPSH for the two kinds of El Niño phases are similar to each other. Therefore, the difference of tracks for the two kinds of El Niño events occurs mainly because there are more TCs forming in the northern tropical WNP during El Niño Modoki years, which chiefly make landfall in the northern coast of China (see green curves in Figure 8).

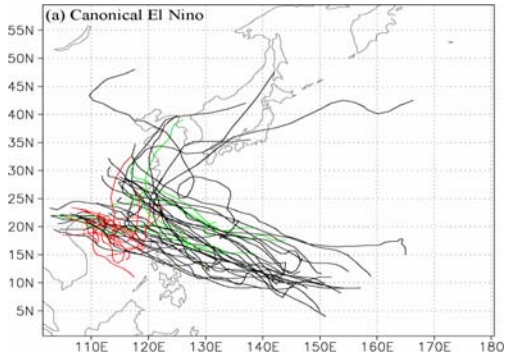

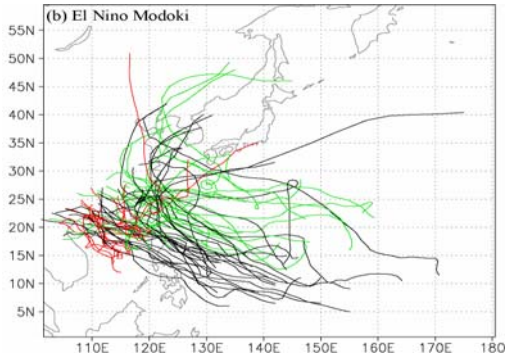

Figure 8. Tracks of TCs that make landfall in China in the two kinds of El Niño phases. Red, green and black curves denote the tracks of landfalling TCs forming in the SCS, the northern tropical WNP and the southern tropical WNP, respectively.

Figure 9 shows the tracks of landfalling TCs in China during the two kinds of La Niña phases. In La Niña Modoki years, TCs make landfall mainly on the southern coast of China. The reason is that the WNPSH is located in the westernmost region reaching the mainland China (Figure 10). This pattern prevents TCs from making landfall on the northern coast of China during La Niña Modoki years. In canonical La Niña years, more TCs make landfall in China, for the WNPSH is more to the east and more TCs generate in canonical La Niña years than in La Niña Modoki years.

In general, since the differences of the locations of WNPSH among canonical El Niño, canonical La Niña and El Niño Modoki years are not evident, the impacts of WNPSH on the tracks in these ENSO

phases are similar. The difference among the tracks in these three ENSO phases is mainly due to the frequencies and genesis locations of landfalling TCs. The WNPSH in La Niña Modoki years is located in the west of the WNPSH in other three ENSO phases which prevent TCs from making landfall on the northern coast of China.

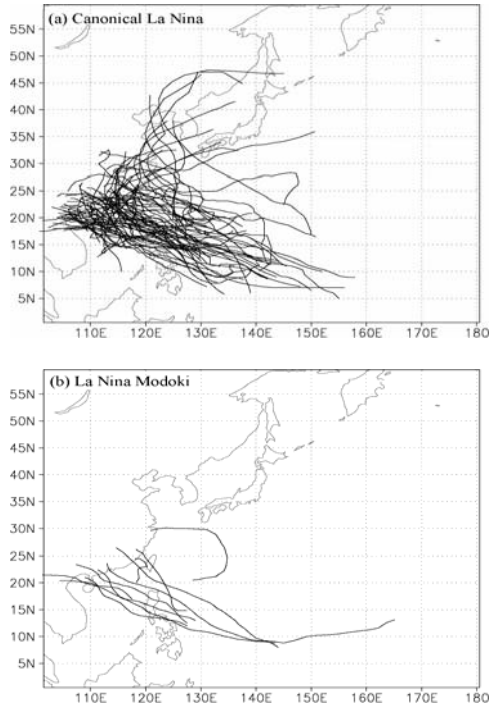

Figure 9. Tracks of TCs that make landfall in China in the two kinds of La Niña phases.

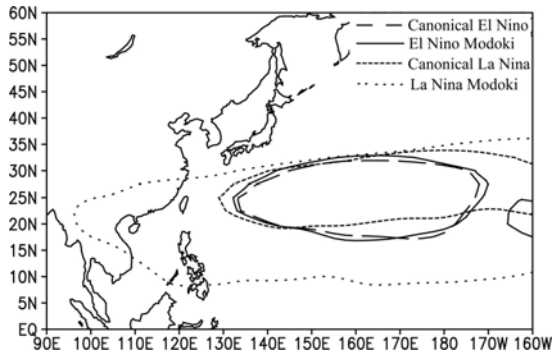

Figure 10. Contours of 5870 gpm at 500 hPa averaged over the typhoon season for each of the ENSO phases. Dashed, solid, short-dashed and dot curves represent canonical El Niño, El Niño Modoki, canonical La Niña and La Niña Modoki years, respectively.

7 CONCLUDING REMARKS

With the method of PLS-regression, the factors that contribute to the interannual variability of landfalling TC frequency in China during the typhoon season of 1960 to 2010 are investigated. The different impacts of canonical ENSO and ENSO Modoki phases on the frequency and tracks of landfalling TCs in China are then examined. The major conclusions are summarized as follows.

(1) The time series of landfalling TC frequency exhibits large interannual variability during 1960 to 2010 in China. The PLS-regression using SST as the predictor field yields two useful patterns with prediction skill. The first pattern is dominated by canonical ENSO while the second resembles ENSO Modoki closely. These two patterns jointly explain 46.7% of the variance of the landfalling TC frequency in China.

(2) El Niño Modoki years are associated with a greater-than-average frequency of landfalling TCs. On the contrary, canonical El Niño years result in diminished TCs making landfall in China. Significant difference of landfalling TC genesis location between the two kinds of El Niño phases is found in the northern tropical WNP. Additionally, more landfalling TCs form in the SCS during El Niño Modoki years, while the frequencies of landfalling TCs are similar in the southern tropical WNP for the two kinds of El Niño phases. As for the two kinds of La Niña phases, there are slightly more landfalling TCs in canonical La Niña years and less landfalling TCs during La Niña Modoki years, compared with the climatological mean. The patterns of OLR anomalies and low-level circulation anomalies are investigated in order to identify the physical mechanism. The results show that during canonical El Niño years, a region of suppressed convection roughly extends from the equator to 25°N except for the southeastern tropical WNP. Correspondingly, the low-level wind anomalies are characterized by a meridionally symmetric dipole pattern with a usual anomalous anticyclone/cyclone near the subtropical/tropical region. In El Niño Modoki years, enhanced convection dominates almost the entire tropical WNP. Additionally, an intensive large-scale anomalous cyclone, with the center near (145°E, 20°N), occupies almost the whole region where landfalling TCs generate. As for the La Niña phases, enhanced convection occurs in the SCS and the west of the tropical WNP, causing landfalling TCs to form more to the west during canonical La Niña years. Meanwhile, an unfavorable condition for TC genesis persists in a broad zonal band from 5°N to 25°N in La Niña Modoki years.

(3) In El Niño phases, more TCs make landfall on the northern coast of China in El Niño Modoki years than in canonical El Niño years. Since the WNPSH of these two El Niño phases are similar, a possible reason is that more landfalling TCs form in the northern tropical WNP during El Niño Modoki years and mainly make landfall on the northern coast of China. In the La Niña phases, the WNPSH in La Niña Modoki years extends to the mainland China, which prevents TCs from making landfall on the northern coast of China.

Finally, considering the increasing trend of El

Niño Modoki events under the background of global warming[15, 31] and the larger potential to make TCs landfall in China during El Niño Modoki years, the impacts of El Niño Modoki are suggested to be considered in statistical prediction for the TCs making landfall in China.

REFERENCES:

[1] CHAN J C L. Tropical cyclone activity over the western North Pacific associated with El Niño and La Niña events [J]. J. Climate, 2000, 13: 2960-2972.

[2] WANG Bin, CHAN J C L. How strong ENSO events affect tropical storm activity over the western North Pacific [J]. J. Climate, 2002, 15: 1643-1658.

[3] WU M C, CHANG W L, LEUNG W M. Impacts of El Niño–Southern Oscillation events on tropical cyclone landfalling activity in the western North Pacific [J]. J. Climate, 2004, 17: 1419 - 1428.

[4] CHIA H H, ROPELEWSKI C F. The interannual variability in the genesis location of tropical cyclones in the northwest Pacific [J]. J. Climate, 2002, 15: 2934-2944.

[5] CAMARGO S J, SOBEL A H. Western North Pacific tropical cyclone intensity and ENSO [J]. J. Climate, 2005, 18: 2996-3006.

[6] CHEN T C, WENG S P, YAMAZAKI N, et al. Interannual variation of the tropical cyclone activity over the western North Pacific [J]. J. Climate, 2006, 19: 5709-5720.

[7] ZHAN Rui-fen, WANG Yu-qing, LEI Xiao-tu. Contributions of ENSO and east Indian Ocean SSTA to the interannual variability of northwest Pacific tropical cyclone frequency [J]. J. Climate, 2011, 24: 509-521.

[8] FENG Li-hua. Relationship between tropical cyclones landing in China and sea surface temperature in the Pacific [J]. Acta Geograph. Sinica (in Chinese), 2003, 58(2): 209-214.

[9] LIN Hui-juan, ZHANG Yao-cun. Climatic features of the tropical cyclone influencing China and its relationship with the sea surface temperatures in the Pacific Ocean [J]. J. Trop. Meteor. (in Chinese), 2004, 20(2): 218-224.

[10] WANG Xiao-ling, SONG Wen-ling. Studies on relationships between ENSO and landfalling tropical cyclones in China [J]. J. Trop. Meteor., 2010, 16(2): 189-194.

[11] TRENBERTH K E, STEPANIAK D P. Indices of El Niño evolution [J]. J. Climate, 2001, 14: 1697-1701.

[12] LARKIN N K, HARRISON D E. Global seasonal temperature and precipitation anomalies during El Niño autumn and winter [J]. Geophys. Res. Lett., 2005, 32: L16705, doi:10.1029/2005GL022860.

[13] ASHOK K, YAMAGATA T. The El Niño with a difference [J]. Nature, 2009, 461: 481-483.

[14] KAO Hsum-ying, YU Jin-yi. Contrasting eastern-Pacific and central-Pacific types of ENSO [J]. J. Climate, 2009, 22: 1499-1515.

[15] ASHOK K, BEHERA S K, RAO S A, et al. El Niño Modoki and its possible teleconnection [J]. J. Geophys. Res., 2007, 112: C11007, doi:10.1029/2006JC003798.

[16] WENG H, ASHOK K, BEHERA S, et al. Impacts of recent El Niño Modoki on dry/wet conditions in the Pacific rim during boreal summer [J]. Clim. Dyn., 2007, 29: 113-129, doi:10.1007/s00382-007-0234-0.

[17] KIM Hye-mi, WEBSTER P J, CURRY J A. Impact of shifting patterns of Pacific Ocean warming on North Atlantic tropical cyclones [J]. Science, 2009, 325: 77-80, doi:10.1126/science.1174062.

[18] CHEN Guang-hua, TAM Chi-yung. Different impacts of two kinds of Pacific Ocean warming on tropical cyclone frequency over western North Pacific [J]. Geophys. Res. Lett., 2010, 37: L01803, doi: 10.1029/2009GL041708.

[19] KIM Joo-hong, HO Chang-hoi, SUI C H. Circulation features associated with the record-breaking typhoon landfall on Japan in 2004 [J]. Geophys. Res. Lett., 2005, 32: L14713, doi:10.1029/2005GL022494.

[20] KALNAY E, KANAMITSU M, KISTLER R, et al. The NCEP/NCAR 40-year reanalysis project [J]. Bull. Amer. Meteor. Soc., 1996, 77: 437-470.

[21] LIEBMANN B, SMITH C A. Description of a complete (interpolated) OLR dataset [J]. Bull. Amer. Meteor. Soc., 1996, 77: 1275-1277.

[22] McINTOSH P C, ASH A J, Stafford S M. From oceans to farms: The value of a novel statistical climate forecast for agricultural management [J]. J. Climate, 2005, 18: 4287-4302, doi:10.1175/JCLI3515.1.

[23] KALELA-BRUNDIN M. Climatic information from tree‐rings of Pinus sylvestris L. and a reconstruction of summer temperatures back to AD 1500 in Femundsmarka, eastern Norway, using partial least squares regression (PLS) analysis [J]. Holocene, 1999, 9: 59-77, doi:10.1191/095968399678118795.

[24] SMOLIAK B V, WALLACE J M, STOELINGA M T, et al. Application of partial least squares regression to the diagnosis of year-to-year variations in Pacific Northwest snowpack and Atlantic hurricanes [J]. Geophys. Res. Lett., 2010, 37: L03801, doi:10.1029/2009GL041478.

[25] SHU Shou-juan, WANG Yuan, XIONG An-yuan. Estimation and analysis for geographic and orographic influences on precipitation distribution in China [J]. Chinese J. Geophys. (in Chinese), 2007, 50 (6): 1703-1712.

[26] ABDI H. Partial least squares regression, projection on latent structure regression (PLS-Regression) [J]. Wiley Interdiscip. Rev. Comput. Stat., 2010, 2: 97-106.

[27] LI Chun-hui, LIU Chun-xia, CHENG Zheng-quan. The characteristics of temporal and spatial distribution of tropical cyclone frequencies over the South China Sea and its affecting oceanic factors in the past 50 yrs [J]. J. Trop. Meteor. (in Chinese), 2007, 23(4): 341-347.

[28] LANDER M A. An exploratory analysis of the relationship between tropical storm formation in the western North Pacific and ENSO [J]. Mon.Wea. Rev., 1994, 122: 636-651.

[29] CHOI Ki-seon, WU Chun-chieh, WANG Yu-qing. Effect of ENSO on Landfalling tropical cyclones over the Korean Peninsula [J]. Asia-Pacific J. Atmos. Sci., 2011, 47(4): 391-397, doi:10.1007/s13143-011-0024-9.

[30] HO Chang-hoi, KIM Joo-hong, KIM Hyeong-seog, et al. Possible influence of the Antarctic Oscillation on tropical cyclone activity in the western North Pacific [J]. J. Geophys. Res., 2005, 110: D18104, doi:10.1029/2005JD005766.

[31] YEH Sang-Wook, KANG Sok-Kuh, DEWITTE B, et al. El Niño in a changing climate [J]. Nature, 2009, 461: 511-514.

Citation: DU Yu-gang, SONG Jin-jie and TANG Jian-ping. Impacts of different kinds of ENSO on landfalling tropical cyclones in China. *J. Trop. Meteor.*, 2013, 19(1): 39-48.